Bull. Chem. Soc. Ethiop. **2023**, 37(5), 1151-1162.
DOI: https://dx.doi.org/10.4314/bcse.v37i5.8

ISSN 1011-3924
Printed in Ethiopia
Online ISSN 1726-801X

SPECTROSCOPIC, THERMAL, AND ANTICANCER INVESTIGATIONS OF NEW COBALT(II) AND NICKEL(II) TRIAZINE COMPLEXES

Amnah Mohammed Alsuhaibani[1], Abdel Majid A. Adam[2*], Moamen S. Refat[2], Mohamed I. Kobeasy[2], Safyah B. Bakare[3] and Eman Salah Bushara[4]

[1]Department of Physical Sport Science, College of Education, Princess Nourah bint Abdulrahman University, P.O. Box 84428, Riyadh 11671, Saudi Arabia
[2]Department of Chemistry, College of Science, Taif University, P.O. Box 11099, Taif 21944, Saudi Arabia
[3]Faculty of Education, Shaqra University, Al Muzahimiyah, Shaqra, Riyadh Province, P.O. Box 205, 11972, Saudi Arabia
[4]Department of Chemistry, Faculty of Education, Alzaeim Alazhari University, Khartoum, Sudan

(Received March 10, 2023; Revised April 4, 2023; Accepted April 5, 2023)

ABSTRACT. The condensation of thiosemicarbazide with oxazolidinone produced 5-benzylidene-3-(4-chloro-phenyl)-6-oxo-5,6-dihydro-1H-[1,2,4]triazine-2-carbothioic acid amide (HL_1). Co(II) and Ni(II) ions were reacted with the HL_1 ligand. Elemental analysis and molar conductivity, along with mass, ^{1}H-NMR, IR, UV-Vis, and X-ray powder diffraction spectral examinations, were used to reveal the chemical structure of the synthesized complexes. The stoichiometry of the complexes was determined to be 1:2 (metallic: moiety) using analytical, spectroscopic, and thermal data. The thermal properties of the complexes were explored using thermogravimetric (TG-DTG/DTA) methods, as well as the decomposition stages. Several kinetic thermodynamic parameters such as free activation energy (ΔG*), activation enthalpy (ΔH*), activation entropy (ΔS*), pre-exponential factor (A), and the activation energy (E*) were estimated. Inhibitory effects towards colon carcinoma cells (HCT cell line), hepatocellular carcinoma (Hep G2 cell line), and breast carcinoma (MCF-7 cell line) were verified using various concentrations of the samples. A colorimetric method was used to determine the cell viability percent in comparison to doxorubicin drug as a control.

KEY WORDS: 1,2,4-Triazines, Thiosemicarbazide, Thermogravimetric analysis, Non-electrolytes, Anticancer

INTRODUCTION

Metallic complexes of S (sulfur) and N (nitrogen) chelating binding moiety have garnered substantial consideration [1] due to their intriguing physical and chemical features, prominent biotic abilities, and as a prototype of dynamic sites of the metallic enzyme. Schiff-base metal complexes have industrial, antimycotic, antimicrobial, anti-malignant, and pesticide uses; therefore, they have been extensively researched. They can be used as a prototype for physiologically significant types and in mimicking biocatalytic methods [2]. Triazine derivatives have long been used as complexing agents in analytical chemistry, as redox systems with several steps in electrochemistry, and as herbicide or pesticide elements in agriculture. They have antitubercular, antimicrobial, antimycotic, antihypertensive, and antipyretic properties [3]. Several 1, 2, 4-triazine-containing compounds have been found in natural materials and have therapeutic, pharmacological, and biological effects [4, 5]. Research [6] used a variety of Zn(II), Cu(II), Ni(II), and Co(II) complexes of bidentate Schiff base produced from the reaction of 4-amino-3-mercapto-6–methyl-5-oxo-[1,2,4] triazine with 5-bromothiophene-2-carboxaldehyde. Reaction of Zn(II), Cu(II), Ni(II), Co(II), Fe(III), and Mn(II) ions with 3-benzyl-7-hydrazinyl-4H-[1,3,4] thiadiazolo[2,3c][1,2,4] triazin-4-one was also described [7]. Researchers investigated

*Corresponding author. E-mail: majidadam@yahoo.com

the complexation of platinum(II) chloride with 4-amino-6-methyl-1, 2, 4-triazine-3-thione-5-one in THF solvent [8]. Complexes of 5,6-diphenyl-3-(2`-hydroxyphenyl)-1,2,4-triazine with Ni(II), 5,6-diphenyl-3-(2-pyridyl)-1,2,4-triazine with Cu(II), and the 2-octylthio-1,3,5-triazine-4,6-dithiolate ion with Pt(II) have been produced and identified [9-12]. The thiosemicarbazide moiety possesses a good chelating ability, which can be augmented in thiosemicarbazone by implanting an appropriate R-CHO or RR-CO with additional giver particles to make the binding moiety polydentate. The large range of potential Schiff bases metallic complexes, as well as the variety of binding moieties and harmonization settings, led us to conduct studies in this field [13]. The work aimed to synthesize and characterize the Co(II) and Ni(II) complexes with HL_1 ligand.

EXPERIMENTAL

Materials

All the materials employed in the current study are of pure grade chemicals. $CoSO_4$ (≥99%) and $NiSO_4$ (99%) hydrate were obtained from "Fluka Chemical Co."

Synthesis of HL_1 ligand

The HL_1 ligand was produced by combining thiosemicarbazide (0.01 mol) with 3-bromo-4-methoxy-benzylidene derivatives (0.01 mol) and oxazolinone in acetic acid (25 mL). The mixture was kept at a high temperature under reflux for 2 hours. After cooling, the resulting solid was crystallized in acetic acid, filtered off, subjected to ethanolic wash, and dried. The HL_1 ligand was obtained as amber crystals with a yield of 78% and a melting point of 160 °C. ^{1}H NMR (DMSO-d_6, ppm) δ: 10.06 (s, 1H, NH), 8.34 (s, 1H, CH=N), 7.24-8.01 (m, 10H, Ar-H and H-olefinic), and 3.36 (s, 2H, NH_2) ppm. IR (KBr) = 3405 and 3188 cm^{-1} (NH_2), 1356 cm^{-1} (thioamide), 3285 cm^{-1} (νNH), 1683 cm^{-1} (νC=O), 1630 cm^{-1} (νC=N), and 1520-1596 cm^{-1} (νC=C).

Synthesis of HL_1 complexes

Free HL_1 ligand (2 mmol) dissolved in hot DMF (20 mL) was mixed with an aqueous solution of the metal salt [Co(II) or Ni(II)] (1.0 mmol, 10 mL). The mixture was heated for 3 hours at temperature 60-70 °C. After allowing the solutions to sit for a night, a pink and light green colorful mixture of Co(II) and Ni(II) complexes was gathered. Filtered solid powder complexes are washed in ethanol and dried over $CaCl_2$. TLC was used to evaluate the purity of the complexes. The melting point of all complexes is above 300 °C.

Physical measurements

Infrared spectra were collected in the 4000–400 cm^{-1} mid-range using a Perkin–Elmer 1420 Spectrometer. The UV–Vis. spectra were obtained in the DMSO solvent with a concentration of ($1x10^{-3}$ M) using a Jenway 6405 Spectrophotometer in the range 200–800 nm. For the freshly produced solutions, molar conductance was measured using a Jenway 4010 conductivity meter at $1x10^{-3}$ mole in DMSO solvent. On General Electric QE 300 equipment, the NMR spectra were acquired, and chemical shifts were calculated in relation to TMS. On Gc/MS with CI (chemical ionization) and a Hewlett–Packard MS–Engine Thermosprary, the mass spectra were obtained. A Shimadzu TGA-50H thermal analyzer was used to perform the thermogravimetric and differential analysis (TGA-DTG/DTA) in an active nitrogen environment.

Assessment of cytotoxic activities of chemical compound

The cytotoxic effects of the tested compounds were evaluated at the Regional Center for Mycology and Biotechnology, Egypt. Trypan blue dyes, crystal violet, and dimethyl sulfoxide (DMSO) were obtained from Sigma Company. Trypsin-EDTA (0.25%), gentamycin, L-glutamine, HEPES buffer solution, RPMI-1640, DMEM, and Fetal Bovine serum were obtained from Lonza Company. All cells were subcultured twice a week and kept in a humidified setting with 5% CO_2 at 37 °C. The cells were planted in 100 µL of growth media, in a 96-well plate at a cell concentration of $1x10^4$ cells per well. The microtiter plates were incubated in a humidified atmosphere with 5% CO_2 at 37 °C for 48 hours. Different quantities of samples (50, 25, 12.5, 6.25, 3.125, and 1.56 µg) were introduced, and the incubation was maintained for two days, with viable cell yield evaluated utilizing a colorimetric method. The absorbance of the plates was dtermined on a Microplate reader (TECAN, Inc.) at 490 nm [14].

RESULTS AND DISCUSSION

The elemental analysis results of the free HL_1 ligand and its Co(II) and Ni(II) complexes are listed in Table 1. Table 1 also indicates several physical and microanalytical characteristics, such as, milting point, color and molar conductance value of the free HL_1 ligand and its Co(II) and Ni(II) complexes. The data shows equimolar stoichiometry (metal: ligand), and the general formula of the complexes based on these results is: $[M(HL_1)_2(SO_4)]$, where M= Co(II) or Ni(II)]. The DMSO solution of Co(II) and Ni(II) complexes (1×10^{-3} M) showed low conductivity. The molar conductance values for these complexes are 49 and 68 cm^2mol^{-1}, respectively. These values indicated the non–electrolytic character of the complexes [15]. The chemical analysis using $BaCl_2$ solution indicated that SO_4^{2-} ion is coordinated to the metal ion.

Table 1. Analytical and physical data for HL_1 ligand, Co (II) and Ni (II) complexes.

Compound (M. Wt.)	M.p. (°C)	Color	$\Omega^{-1}cm^2mol^{-1}$	Elemental analysis (%) found (calculated)			
				C	H	N	M
HL_1 (356.83)	160	Yellow	34	56.97 (57.22)	3.63 (3.67)	15.60 (15.70)	-- (--)
Co(II) complex (868.65)	>300	Pink	49	46.93 (47.01)	3.00 (3.02)	12.54 (12.90)	6.44 (6.78)
Ni(II) complex (868.41)	>300	Light green	68	46.91 (47.02)	2.97 (3.02)	12.45 (12.90)	6.69 (6.76)

Infrared spectra

Table 2 states the diagnostic IR spectral bands of the HL_1 ligand and its complexes, as well as their preliminary designations. Table 2 shows the IR spectral data of the Co(II) and Ni(II) complexes with their corresponding vibrational bands. The IR spectrum of free HL_1 ligand shows varied intensity from fade-to-moderate strength absorbance bands at 3405 and 3188 cm^{-1} (NH_2). The band at 1356 cm^{-1} was attributed to thioamide vibrations [15]. The presence of distinct thioamide bands in the HL_1 free binding moiety, on the other hand, implies the existence of free-binding moiety in the thione form. The ν(NH) vibrational band for the free ligand was classified into the fade-to-moderate strength bands at 3285 cm^{-1}. The vibration movements of ν(C=O) bands for the ligand are allocated to the refereed band at 1683 cm^{-1}. A strong band of about 1630 cm^{-1} was also ascribed to the triazine ring's ν(C=N) ring. Both phenyl rings had aromaticity bands of ν(C=C) in the range of 1520-1596 cm^{-1}. In the IR spectra of the synthesized complexes, the absence of thioamide bands, particularly the ν(C=S) (1350 cm^{-1}) band, and the greater shift of the ν(NH) band suggested that they were involved in coordination.

Table 2. Assignments of main IR spectral bands (cm^{-1}) of HL_1, Co (II) and Ni (II) complexes.

Compound	ν(NH_2)	ν(NH)	ν(C=O)	ν(C=N)	ν(C=C)	ν(C=S)
HL_1	3405 3188	3285	1683	1633	1596 1520	1356
Co(II) complex	3375 3196	--	1649	1649	1507	--
Ni(II) complex	3341	--	1654	1654	--	--

Molar conductivity

The DMSO solution of Co(II) and Ni(II) complexes (1×10^{-3} M) showed low conductivity. The molar conductance of the synthesized complexes (Table 1) was found to be between 49 and 68 cm^2mol^{-1}. These values indicated the non–electrolytic character of the complexes [16]. The deprotonated character of the ligand in most complexes, as well as the covalent attachment of SO_4 to the metallic cations, account for the complexes' neutrality. This confirmed that the anions of these complexes are coordinated with the metal ion. This result was strongly supported by the chemical analysis, where SO_4^{2-} ion is detected by the addition of $BaCl_2$ solution.

Electronic spectra

When the electronic spectra of the free HL_1 ligand are compared to those of their corresponding Co(II) and Ni(II) complexes, certain changes are visible, which can be taken as a sign for complex creation. These bands emerged at 285 and 415 nm in neutral moderate for free binding moieties. These bands are thought to be caused by π→π* and n→π* transitions inside the functional binding moieties. In addition, metal complexes' absorption spectra (in DMSO) contain additive bands at distinct wavelengths. The Ni^{II} complexes absorbance spectral revealed two distinct bands at 680 and 500 nm, which were ascribed to the transitions $^3A_{2g}(F) \rightarrow {}^3T_{1g}(P)$, and $^3A_{2g}(F) \rightarrow {}^3T_{1g}(F)$, respectively. The octahedral geometry of the Ni^{II} complex is suggested by its spectra. As a result of $^4T_{1g}(F) \rightarrow {}^4T_{2g}(P)$, $^4T_{1g}(F) \rightarrow {}^4A_{2g}(F)$, $^4T_{1g}(F) \rightarrow {}^4T_{2g}(F)$, the electronic spectrum of the octahedral Co^{II} complex has three types of transitions at 790, 631, and 539 nm, respectively. Based on the preceding explanation, Figure 1 is proposed.

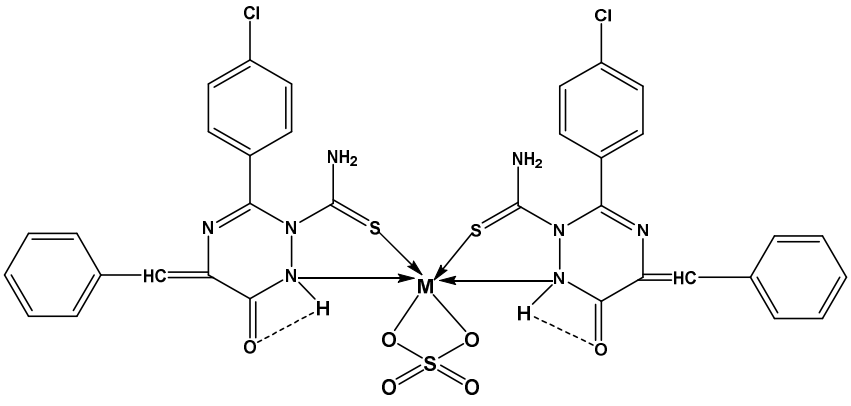

Figure 1. The proposed chemical structures of the Co(II) and Ni(II) complexes [M = Ni(II) and Co(II)].

Mass spectra

The mass spectral of HL_1 indicated a powerful ion peak at m/z 356, which corresponds to the chemical formula $C_{17}H_{13}N_4ClOS$. By removing the NHCS group, the ion of HL_1 (Figure 2) fragmented to create a peak at m/z 297. The ion with m/z 297 lost its NH group, resulting in an ion with m/z 282, which lost its C=O to provide a peak at m/z 254. The ion at m/z 254 was fragmented, resulting in a stable peak at m/z 117. The hydrogen cyanide (HCN) and acetylene molecules in the ion at m/z 117 were lost, resulting in peaks at m/z 64 and m/z 90. The ion at m/z 254 was also fragmented and rearranged, yielding a signal at m/z 139. The chlorine atoms, hydrogen cyanide, and hydrogen atom were lost from the ion at m/z 139, resulting in peaks at m/z 76, m/z 111, and m/z 158, respectively. MS data of HL_1 molecule m/z (%): 50(15.80), 51(15.50), 63(14.10), 64(34.30), 65(4.80), 74(9.70), 75(38.40), 76(24.30), 77(6.50), 89(27.60), 90(23.90), 91(4.40), 100(2.20), 101(4.80), 103(6.10), 104(2.80), 105(1.70), 116(23.20), 117(100.00), 118(9.90), 119(1.40), 137(20.20), 138(44.40), 139(13.70), 140(16.70), 140(16.70), 140(16.70), 141(5.20), 152(2.70), 153(24.10), 154(3.60), 155(7.80), 176(1.30), 177(1.10), 178(1.20), 179(1.30), 194(1.80), 195(3.20), 197(1.30), 203(1.70), 204(1.00), 281(17.10), 283(12.20), 284(14.80), 296(7.50), 297(9.40), 298(3.40), 299(3.40), 338(5.40), 339(7.90), 340(2.70), 355(M^+-1, 5.60), 356(M^+, 7.70), 357(M^++1, 3.20), and 358(M^+ +2, 3.10).

Thermo gravimetric analysis

Figure 3 A-C shows the thermal decomposition curves (TG weight loss data/peak temperatures of DTG and DTA). The HL_1 ligand is degraded in five stages. The first stage begins at roughly 30° and ends at 100°. DTA and DTG maxima appear at 55 and 53 °C, correspondingly, with roughly similar data for this stage. Organic classes, such as $C_{11}H_{13}ClN_4OS$, develop. This stage is responsible for 81.71% of weight loss. Around 800 °C, the first stage has ended. The entire mass reduction calculated is 79.82%. For these phases, there are 5DTG and 4 DTA peaks at (53, 157, 214, 317, and 570 °C), and (55, 246, 383, and 576 °C). The entire decomposition procedure concludes with very little carbon behind it. At temperature, the Co(II) complex begins to lose. The loss of terminal molecules accounts for 29.0% of the mass loss in the first stage (30-119 °C). The TG results are supported by a single medium peak for DTG at 104 °C, which was assigned to liberate one NH_2 molecule and one chlorine atom. The residual complex begins to decompose around 120 °C, and the partial structure is destroyed at 800 °C. Many tiny gas molecules are liberated at this moment. Two DTG peaks (329, 784 °C) and three DTA peaks (60 °C (endo), 337 °C (endo), 520 °C (endo)) may be seen for this phase, indicating that at least three intermediary steps are created during this degradation stage. This stage is responsible for weight loss (reported to be 55.23%). CoO contaminated with carbon atoms is recognized as the final stable residue after 800 °C. At 30 °C, the Ni(II) complex begins to lose mass and shows four breakdown phases. Five DTG (64, 288, 364, 498, and 757 °C) and two obvious DTA (67 (endo), and 757 °C (endo)) are used in these phases. It's worth noting that the ligand decomposes in two steps when complexed with Ni(II), whereas it pyrolyzes in four steps when decomposed alone. The loss of terminal groups for the organic moiety of the HL_1 ligand, which accounts for 14.12% weight loss, is attributable to the first stage, which leaves the other organic portion connected with nickel ions behind. The ligand from labor separates in an unexpected way from the second to fourth breakdown phases, losing 48.95% of its mass. Nickel oxide (NiO) polluted with a few carbon atoms, is the ultimate remaining product of the Ni(II) complex.

Kinetic studies

The kinetic characteristics of the decomposition processes were elucidated using different kinetic approaches such as Horowitz-Metzger (HM) and Coats-Redfern (CR) [17, 18]. The foregoing approaches were used to compute parameters such as Gibbs free energy change; ΔG^*, enthalpy

change; ΔH*, entropy change; ΔS*, frequency factor; A, and activation energy; E (Figure 4). Each method's activation energy values were in good agreement with one another.

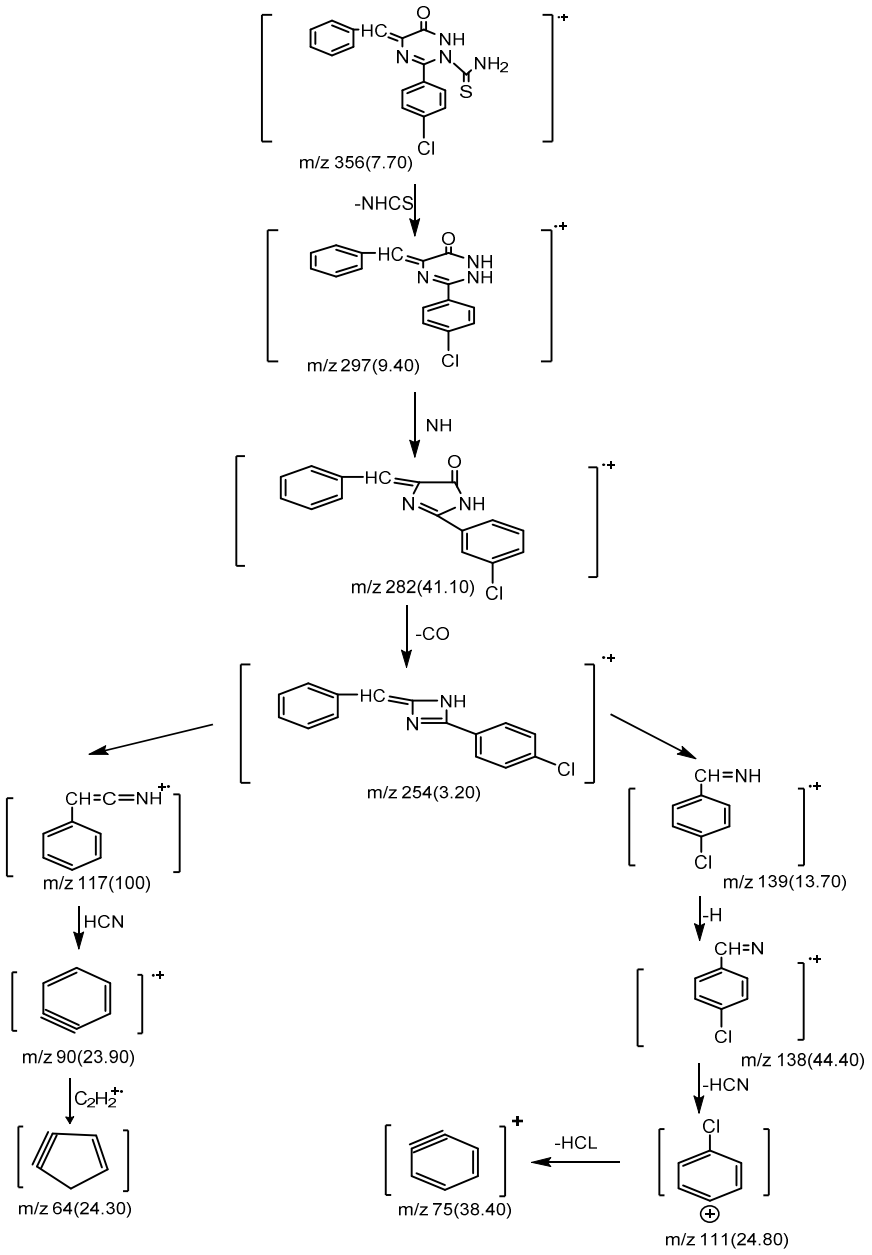

Figure 2. Proposed fragmentation pathways of free HL_1 ligand.

The thermogravimetric study was also used to find an appropriate mechanism for each material's thermal degradation process. Table 3 lists the computed thermodynamic parameters from TG and DTG. The order parameter for the decomposition stage of interest was chosen as the n value that offered the greatest fit ($r \approx 1$). The A and E values were calculated using the intercept and linear slope of such a stage. The following points should be noted: (i) All phases of complex decomposition have a best fit for ($n = 1$), suggesting that they are all first-order decompositions. (ii) Negative activation entropies ΔS suggest that the activated complexes are more ordered than the reactants and that the reactions are sluggish. (iii) ΔH values are positive indicate that the breakdown processes are endothermic.

Table 3. Kinetic parameters using HM and CR methods operated for HL_1 ligand, Co(II) and Ni(II) complexes.

Compound	Method	Kinetic parameters					
		E ($Jmol^{-1}$)	A (S^{-1})	Δ S ($Jmol^{-1}K^{-1}$)	Δ H ($Jmol^{-1}$)	Δ G ($Jmol^{-1}$)	r
HL_1	CR	4.86E+04	1.15E+02	-2.11E+02	4.39E+04	1.62E+05	0.99671
	HM	6.01E+04	2.23E+03	-1.86E+02	5.54E+04	1.60E+05	0.99922
Co(II) complex	CR	8.07E+04	7.86E+10	-3.70E+01	7.81E+04	9.00E+04	0.9955
	HM	8.65E+04	2.43E+12	-8.49E+00	8.39E+04	8.66E+04	0.9923
Ni(II) complex	CR	8.05E+04	2.84E+03	-1.86E+02	7.46E+04	2.67E+05	0.9995
	HM	1.03E+04	2.30E+05	-1.50E+02	9.75E+04	2.04E+04	0.9998

XRD study

Powder X-ray diffraction (XRD) data prpoased a monoclinic structure for the HL_1 ligand and its Ni(II) and Co(II) complexes (Figure 5). The mean crystallite sizes of the free ligand and its complexes (D) were calculated using the Scherrer equation [$D = 0.9\lambda/(\beta \cos\theta)$], where β is the full width at half maximum of the diffraction peak), θ is Bragg diffraction angle, and λ is X-ray wavelength (1.5406 Å). The average crystallite sizes of all compounds were found to be ~ 23–37 nm.

Cytotoxicity studies

The cytotoxic and anticancer effects of the HL_1 ligand and its Co(II) and Ni(II) complexes against cell lines MCF-7, Hep G2, and HCT were tested according to MTT assay [19]. Different concentrations of the tested compound were used and cell viability (percent) was evaluated using a colorimetric method. The cytotoxicity results were listed in Table 4. Table 5 summarizes the results of the 50% inhibitory concentration (IC_{50}) data. The HL_1 ligand was found to be active against HCT, HePG-2, and MCF-7 cell lines when compared to the standard anticancer medication doxorubicin. MCF-7, HePG-2, and HCT cell lines were also reported to be active against Co(II) and Ni(II) complexes. The cytotoxic activity results reveal that the Co(II) and Ni(II) complexes show fairly less activity against all the tested MCF-7, HCT, and HePG-2 cell lines, and in general, the activity order of the compounds can be represented as HL_1 > Ni(II) > Co(II). The higher activity of the free HL_1 ligand in comparison with the metal complexes may be owing to the effect of metal ions on the normal cell membrane [20]. The synthesized complexes display marked cytotoxic activity against the tested cancer cell lines (MCF-7, HCT, and HePG-2), and the IC_{50} values for the complexes were decreased compared with that of the free HL_1.

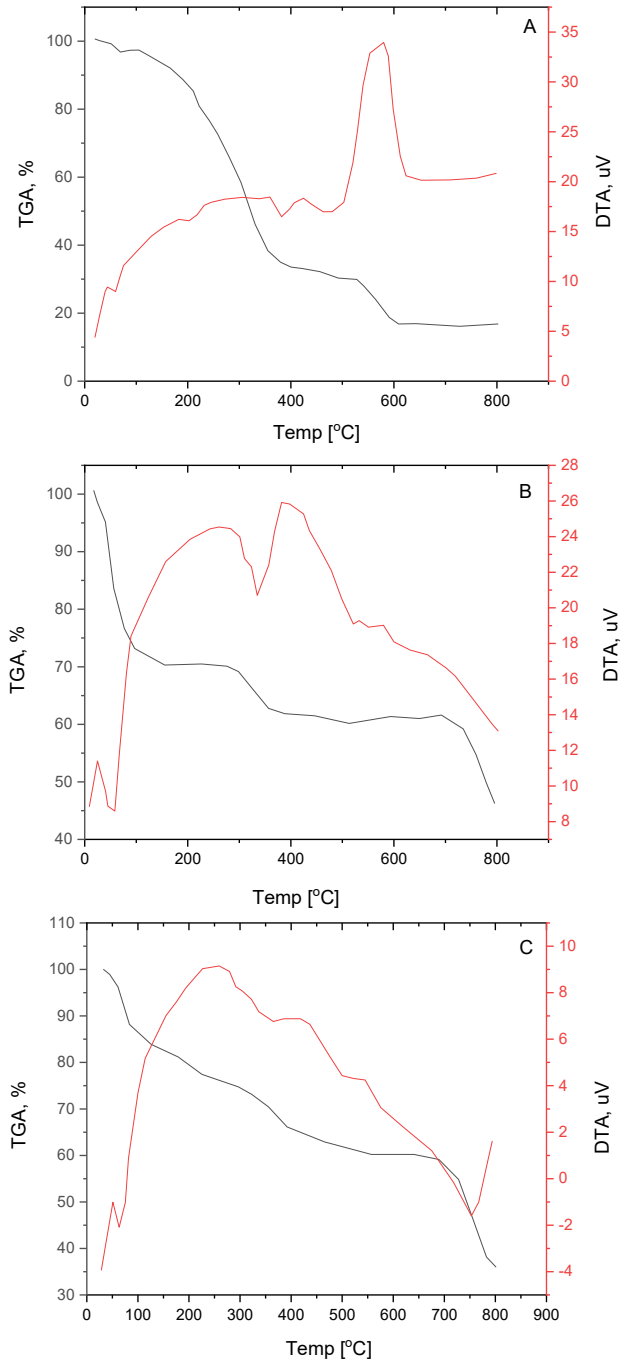

Figure 3. TG-DTG-DTA curves of A; free HL_1, B; Co(II) complex, and C; Ni(II) complex.

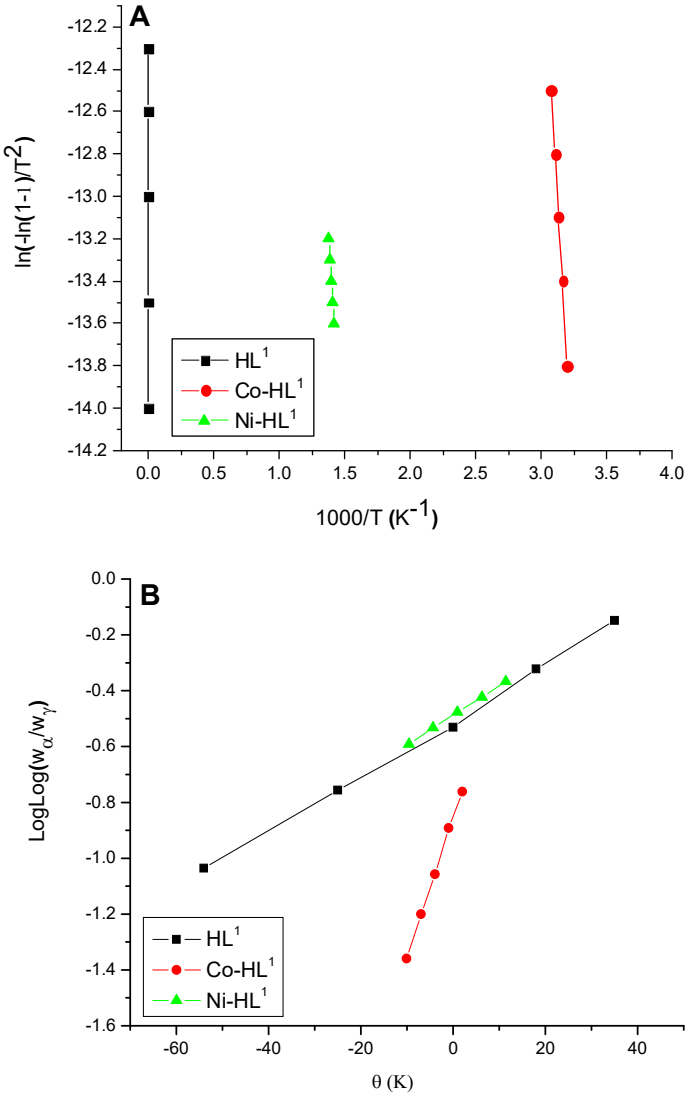

Figure 4. Coats-Redfern (A) and Horowitz-Metzger (B) curves of HL_1, Co(II), and Ni(II) complexes.

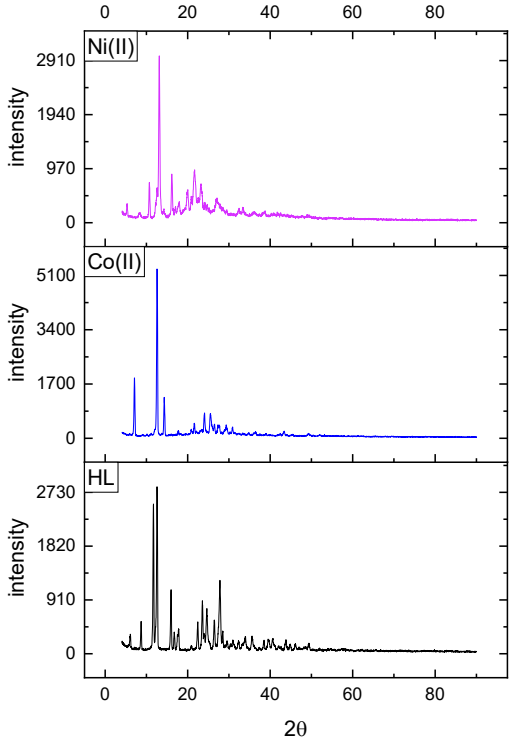

Figure 5. XRD spectra of HL_1, Co(II) and Ni(II) complexes.

Table 4. Cytotoxicity results of HL_1 ligand and its complexes against HCT, HePG-2, and MCF-7 tumor cell lines.

Sample conc. (µg)	Viability % of tumor type/cell line								
	MCF-7			HePG-2			HCT		
	HL_1	Co(II)	Ni(II)	HL_1	Co(II)	Ni(II)	HL_1	Co(II)	Ni(II)
50	4.35	43.38	71.24	4.22	78.14	41.73	4.89	73.82	58.92
25	8.13	77.14	83.18	8.93	89.93	56.84	9.48	90.36	71.38
12.5	10.98	86.19	94.95	11.71	97.18	70.96	13.17	98.43	85.29
6.25	17.45	95.75	98.47	18.25	100.00	88.53	24.36	100.00	94.61
3.125	23.17	98.97	100.00	31.74	100.00	96.32	33.71	100.00	98.73
1.56	38.59	100.00	100.00	50.42	100.00	100.00	41.19	100.00	100.00
0.78	49.73	100.00	100.00	58.14	100.00	100.00	52.83	100.00	100.00
0.39	61.18	100.00	100.00	67.58	100.00	100.00	60.92	100.00	100.00
0	100.00	100.00	100.00	100.00	100.00	100.00	100.00	100.00	100.00

Table 5. IC_{50} (µg) values for HL_1 ligand and its complexes.

Compound	Tumor type/cell line		
	HCT	HePG-2	MCF-7
HL_1	1.00	1.60	0.80
Co(II) complex	50	50	45.1
Ni(II) complex	50	36.3	50
Doxorubicin standard	0.469	1.20	0.426

CONCLUSION

The present report is concerned with the synthesis of two metal complexes of HL_1 ligand. The free HL_1 ligand was characterized by elemental analysis, infrared, proton NMR, and mass spectrometry. The ligand has got —C=S and N—triazine moieties which are capable of chelation. The synthesized complexes were characterized by magnetic susceptibility, conductance measurements, infrared spectroscopy, and elemental analysis. Infrared spectra suggested that the HL_1 ligand complexed with Co(II) and Ni(II) ions through sulfur of thione and nitrogen of triazine moieties. HL_1 molecule acts as a bidentate ligand and the synthesized complexes have the general formula: $[M(HL_1)(SO_4)]$. To evaluate the in vitro anti-cancer activities of the free ligand and its complexes, the ligand, Co(II), and Ni(II) complexes were tested against HCT, HePG-2, and MCF-7 cell lines. The impact of the free HL_1 and its complexes on the reduction of tumor volume was determined.

ACKNOWLEDGMENT

The researchers would like to acknowledge Deanship of Scientific Research, Taif University for funding this work.

REFERNCES

1. Chohan, Z.H.; Farooq, M.A.; Scozzafava, A.; Supuran, C.T. Antibacterial Schiff bases of oxalyl-hydrazine/diamide incorporating pyrrolyl and salicylyl moieties and of their zinc(II) complexes. *J. Enzyme Inhib. Med. Chem.* **2022**, 17, 1-7.
2. Canpolat, E.; Kaya, M. Studies on mononuclear chelates derived from substituted Schiff-base ligands (Part 2): Synthesis and characterization of a new 5-bromosalicyliden-*p*-aminoacetophenoneoxime and its complexes with Co(II), Ni(II), Cu(II) and Zn(II). *J. Coord. Chem.* **2004**, 57, 1217-1223.
3. Temel, H.; İlhan, S.; Şekerci, M. Synthesis and characterization of a new bidentate Schiff base and its transition metal complexes. *Synth. React. Inorg. Met. Org. Chem.* **2001**, 32, 1625-1634.
4. Uma, R.; Palaniandavar, M.; Butcher, R.J. Synthesis, structure, spectra and redox interconversions in copper(II) complexes of 5,6-diphenyl-3-(2-pyridyl)-1,2,4-triazine. *J. Chem. Soc., Dalton Trans.* **1996**, 10, 2061-2066.
5. Béreau, V.; Marrot, J. Coordination studies of 5,6-diphenyl-3-(2-pyridyl)-1,2,4-triazine towards Zn^{2+} cation. Synthesis and characterization by X-ray diffraction and spectroscopic methods. *Comptes Rendus Chim.* **2005**, 8, 1087-1092.
6. Singh, K.; Kumar, Y.; Puri, P.; Sharma, C.; Aneja, K.R. Thermal, spectral, fluorescence, and antimicrobial studies of cobalt, nickel, copper, and zinc complexes derived from 4-[(5-bromo-thiophen-2-ylmethylene)-amino]-3-mercapto-6-methyl-5-oxo-[1,2,4]triazine. *Inter. J. Inorg. Chem.* **2012**, 2012, 873232.
7. Mohamed, G.G.; Badawy, M.A.; Omar, M.M.; Nassar, M.M.; Kamel, A.B. Synthesis, spectroscopic, thermal and biological activity studies on triazine metal complexes. *Spectrochim. Acta* A **2010**, 77, 773-781.
8. Ghassemzadeh, M.; Mirza-Aghayan, M.; Neumuller, B. Syntheses and characterization of the first platinum complex and new palladacycles of N,S-chelating agent in "triplex" form: Molecular structures of $[(AMTTO)PtCl_2]_3 \cdot 4.5THF$ and $[(AMTTO)PdX_2]_3 \cdot 8MeOH$ (X = Cl and Br) (AMTTO = 4-amino-6-methyl-1,2,4-triazine-3-thione-5-one). *Inorg. Chim. Acta* **2005**, 358, 2057-2065.
9. Zhang, H.X.; Kato, M.; Sasaki, Y.; Ohba, T.; Ito, H.; Kobayashi, A.; Chang, H.C.; Uosaki, K. Terpyridine platinum(II) complexes containing triazine di- or tri-thiolate bridges: Structures, luminescence, electrochemistry, and aggregation. *Dalton Trans.* **2012**, 41, 11497-11506.

10. Bereau, V.; Rey, J.; Deydier, E.; Marrot, J. Synthesis and characterization of new copper(II) and nickel(II) complexes of 3-(2′-hydroxyphenyl)-1,2,4-triazine derivatives. *Inorg. Chim Acta* **2003**, 351, 389-394.
11. Singh, K.; Barwa, M.S.; Tyagi, P. Synthesis and characterization of cobalt(II), nickel(II), copper(II) and zinc(II) complexes with Schiff base derived from 4-amino-3-mercapto-6-methyl-5-oxo-1,2,4-triazine. *Eur. J. Med. Chem.* **2007**, 42, 394-402.
12. Samii, R.; Zanders, D.; Buttera, S.C.; Kessler, V.; Ojamäe, L.; Pedersen, H.; O'Brien, N.J. Synthesis and thermal study of hexacoordinated aluminum(III) triazenides for use in atomic layer deposition. *Inorg. Chem.* **2021**, 60, 4578-4587.
13. Majumder, A.; Chaudrary, C.R.; Mitra, S.; Dahlenburg, L. One novel Cu(II)–amino acid Schiff base complex derived from salicylaldehyde and L-serine: Identification of unusual monodentate 4,4′-bipyridine. *Struct. Chem.* **2005**, 16, 611-616.
14. Vijayan, P.; Raghu, C.; Ashok, G.; Dhanaraj, S.A.; Suresh, B. Antiviral activity of medicinal plants of Nilgiris. *Indian J. Med. Res.* **2004**, 120, 24-29.
15. Franco, E.; Lopez-Trorres, E.; Mendiola, M.A.; Sevilla, M.T. Synthesis, spectroscopic and cyclic voltammetry studies of copper(II) complexes with open chain, cyclic and a new macrocyclic thiosemicarbazones. *Polyhedron* **2000**, 19, 441-451.
16. Filo, J.J.; Terron, A.; Mulet, D.; Merno, V. Some new derivatives of Co(III) with uracil, uridine and pyrimidine nucleotides. *Inorg. Chim. Acta* **1987**, 135, 197-202.
17. Coats, A.W.; Redfern, J.P. Kinetic parameters from thermogravimetric data. *Nature* **1964**, 201, 68-69.
18. Horowitz, H.H.; Metzger, G. A new analysis of thermogravimetric traces. *Anal. Chem.* **1963**, 35, 1464-1468.
19. Mohamed, F.H.; Shalaby, A.; Abdelazem, A.; Mounier, M.; Nossier, E.; Moustafa, G. Design, synthesis, and molecular docking studies of novel cyclic pentapeptides based on phthaloyl chloride with expected anticancer activity. *Egyptian J. Chem.* **2020**, 63, 1723-1736.
20. Dharmaraj, N.; Viswanathamurthi, P.; Natarajan, K. Ruthenium(II) complexes containing bidentate Schiff bases and their antifungal activity. *Transit. Metal Chem.* **2001**, 26, 105-109.